NASA Technical Memorandum 81675

Composite Containment Systems for Jet Engine Fan Blades

G. T. Smith
Lewis Research Center
Cleveland, Ohio

Prepared for the
Thirty-sixth Annual Conference of the
Reinforced Plastics/Composites Institute of the
Society of the Plastics Industry, Inc.
Washington, D.C., February 16-20, 1981

NASA

COMPOSITE CONTAINMENT SYSTEMS FOR JET ENGINE FAN BLADES

by G. T. Smith*

National Aeronautics and Space Administration
Lewis Research Center
Cleveland, Ohio 44135

ABSTRACT

This paper summarizes a program to facilitate the use of composites in fan blade containment systems and to identify the associated structural benefits of the composite system design. Results obtained show that a substantial reduction in the fan blade containment system weight is possible. Minimization of damage within the engine arising from impact interaction between blade debris and the engine structure is also achieved.

INTRODUCTION

The development of technology which is required to improve the durability and the structural efficiency of modern aircraft turbine engine systems is the principal objective of a recently expanded engine structures program at the NASA Lewis Research Center. The implementation of this objective involves a series of coordinated programs among Lewis in-house, industrial, and university research organizations. These programs include substantial efforts to exploit the unique mechanical and manufacturing characteristics of advanced composite material systems. These materials, properly characterized and applied, can provide weight efficient design alternatives for several important engine components. Among the most attractive applications for these composite materials is the fan blade containment system.

All commercial aircraft engines are required by Federal Aviation Administration regulations to contain within the nacalle any debris originating from fan blade failure. Except for the relatively rare incidents involving fan blade failures, the fan blade containment case weight is a nonfunctional parasitic weight increment. On a modern large high-bypass aircraft engine, this weight can be in excess of 450 pounds. These systems currently make use of high strength steel for the containment casing surrounding the fan blades. Although effective in preventing escape of fan blade debris, these steel rings provide no significant nesting capability or trajectory control for blade fragments and accordingly tend to rebound the fragments and maximize the interaction between the failed fan blade and trailing rotor blades, thereby increasing engine damage. The program described in this paper was directed towards development of a reliable fan blade containment system which would both minimize engine damage and lower the weight required for effective debris containment.

*Structures Research Engineer, Structures and Mechanical Technologies Division, Lewis Research Center, Cleveland, Ohio.

E-700

CONTAINMENT CONCEPT EVALUATIONS

A variety of lightweight containment concepts were evaluated under contract for NASA. Two contracts were conducted with the General Electric Company to accomplish the programs described by this paper. The initial concept screening process was accomplished with subscale static test specimens which were impacted by projectiles launched from a large bore (4-in. diam) light gas gun. Both the light gas gun equipment and the basic design features of the subscale test specimens had been previously established during an in-house program. This program is described in General Electric Company TIS Report No. 695DB, July 1969 "New Developments in Rotor Containment Technology by A. P. Copper and H. W. Semon.

The gas gun and the containment test specimen arrangement are illustrated in Fig. 1 and are described in detail in Ref. 1. The projectile was mounted on a wooden sabot so that the impact angle between the projectile and the semicircular test specimen was closely controlled. The impact interaction between the simulated blade projectile and the containment test section was recorded by a highspeed motion picture camera. The gas gun facility was capable of muzzle velocities up to about 1000 feet per second. A more detailed view of a containment section target is shown in Fig. 2. The projectile impacted the upper right hand part of the target. The grid lines on the background plate facilitated analysis of the interaction process from the motion picture film. Two types of simulated blade projectiles were used and are illustrated in Fig. 3. The base line configuration was an all titanium projectile 5 inches long by 2 inches wide with a maximum thickness at the midchord of 0.1 inch. The second projectile configuration was intended to simulate the impact characteristics of a superhybrid fan blade and consisted of 0.006-inch titanium foil surrounding a graphite/epoxy core material. Two additional layers of the 0.006-inch titanium were embedded in the leading edge portion of the projectile to simulate the impact effect of a leading edge protection system. A detailed description of the superhybrid composite construction can be found in Ref. 2.

Two basic types of containment structures were investigated and are illustrated in Fig. 4. The short finned concept was evaluated using Kevlar/epoxy laminates for fins which were mounted in a 6061 T-6 aluminum ring. The long fin concept was evaluated with Kevlar/epoxy, 6Al4V titanium, and 2024 T-3 aluminum fins. The unfinned configurations consisted of the base-line steel sheet, a circumferentially oriented aluminum honeycomb, and a Kevlar cloth filled ring. The Kevlar cloth concept was evaluated with both a thin steel and an aluminum face sheet on the impact side.

The gas gun impact test program is summarized in Table I. Twelve of the 20 tests resulted in capture of the impacting projectiles. The four steel band tests resisted penetration and redirected the projectile. The superhybrid projectiles were readily contained by all the systems due to the frangible nature of the composite system under severe impact loading conditions. Figure 5 shows the effective containment and nesting of a superhybrid blade on test number 5. Containment and nesting of the titanium blades was most effectively accomplished by Kevlar belt systems. The best performance was achieved on test number 18 where partial penetration of the containment system occurred but the projectile was retained within the Kevlar cloth indicating the penetration threshold of the system was very nearly realized on that test. A containment performance parameter (contained impact energy divided by system weight per square foot) of 863 ft^3

was achieved. Figure 6 shows the pull out and incipient penetration of the Kevlar belt occurring on test number 18.

The containment thickness requirement of the Kevlar belt system was expected to depend on the impact energy to the one half power. This expectation was based on armour penetration tests conducted by the U.S. Army at the Watertown Arsenal.** Figure 7 illustrates this assumed relationship between Kevlar thickness and projectile kinetic energy. Using test number 18 as representing the penetration threshold provided the expression

$$t = 0.00341\ (E)^{1/2} \qquad (1)$$

where t is measured in inches and E is measured in foot pounds. This condition is represented by the upper curve of Fig. 7. A less conservative estimate based on test number 19 is represented by the lower curve which is defined by a value of 0.00265 for the correlation constant of Eq. (1).

Based on the gas gun test program, a containment concept was evolved for evaluation using full scale TF-34 titanium blades and rotor. The test series consisted of four all titanium and four superhybrid composite blades. The TF-34 fan disk was mounted in a TF-39 fan frame and was driven by an electric motor through a dynamic clutch. The containment system was mounted inside a test chamber which was filled with helium gas during the tests in order to reduce temperature build up within the chamber and to reduce the power requirement for the drive motor. Figure 8 provides a schematic of the test chamber. The containment system interaction with the released blades was recorded by high speed motion picture cameras. The containment system test specimens were fabricated in two 180 degree segments which were attached at two vertically opposed hard points. Four runs were made with two blades being released on each run. The blade release was timed so that each blade fragment impacted approximately in the center of the test sections. A series of radially spaced aluminum witness plates surrounded the test specimens to permit estimation of the residual energy of any debris which penetrated and escaped the containment system.

SPIN IMPACT TEST EVALUATIONS

The Kevlar belt containment system concept selected for rotating test evaluation is shown schematically in Fig. 9. The system was evaluated both with and without a two inch layer of 2.1 pound per cubic foot aluminum honeycomb. The aluminum honeycomb thickness was selected to provide a nesting region for the all-titanium TF-34 blade outside of the normal path of the fan rotor blades. In the design of the test specimens, no contribution to the containment capability was assumed for the honeycomb section or the encasement sheets of steel and aluminum. Since both all-titanium and superhybrid blades were to be evaluated, different thicknesses of Kevlar were required. Table II presents the test sequence and indicates the principal features of the test specimens. All tests were conducted at 5000 rpm. The containment specimens for the superhybrid blades had 22 plies of dry Kevlar and the specimens for the higher energy all-titanium blades had 29 plies. These thicknesses were selected to provide marginal con-

**These data are documented in an internal General Electric Company Report R59SE59 "T-58-GE-6 Turbine Integrity" 5-29-59.

tainment at 5000 rpm. The steel face sheet was 0.020-inch thick and the outer aluminum sheet was 0.032-inch thick for all specimens. Tests were conducted both with and without adjacent trailing blades to isolate the effect of blade interactions on the penetration process and the containment requirements. A total of eight blade impacts were obtained with four spin tests by releasing two diametrically opposite blades on each test. The impact test specimens consisted of two 180 degree segments which were individually attached to vertically opposed hard points. Figure 10 shows a typical test set up (in this case test 4). The rotor turns in a counter clockwise direction. The blades which were impacted into the containment section are shown in Fig. 11. The blade release was accomplished by explosive charges located in machined grooves. The charges were positioned either just above or just below the base platform depending on the weight of the impact fragment desired.

The impact event coverage provided by the high speed movies was crucial to a clear analysis of the performance of the containment system. Figure 12 illustrates the post test condition of the first rotating test. This run was conducted with superhybrid blades impacting 22 ply Kevlar belt systems. Three all-titanium trailing blades were mounted immediately behind the superhybrid test blades so that effects of trailing blade interaction would be incorporated into the test results. Observation of the film established that the explosive charges fired at the proper time but did not sever the titanium spars. The composite portion of the blades separated quickly and one spar separated on the second revolution. The second spar separated on the sixth revolution after interacting with the Kevlar which was being dragged from the right hand containment specimen. Both spars impacted the right hand specimen. The interaction between the Kevlar and the remaining all-titanium blades became strong enough to fracture one of the blades at the root. This fragment weighing 1.3 pounds impacted the left hand section at 4630 rpm. The calculated impact energy of this fragment was 8830 foot pounds which was well above the design containment capability of this test specimen. All of the titanium debris fragments caused rupture of the aluminum outer wall but no fragments impinged upon the witness plates. This test provided a clear demonstration of the necessity of an adequate separation and support of the Kevlar containment belt to prevent interaction with the remaining rotor blades.

The second superhybrid blade test was identical to the first except that no trailing blades were mounted on the rotor thus eliminating any influence of blade debris interaction on the fragment penetration process. The explosive charges again failed to properly separate the blade spars. The composite shells separated and were contained. The spars separated several revolutions later. The spar which impacted the containment section without the honeycomb was contained but rebounded back into the rotor path. The other spar penetrated the honeycomb of the other containment specimen interacted with the Kevlar, and stopped within its own length completely nested outside the path of the rotor. Tests 3 and 4 were conducted with all-titanium blades and 29 plies of Kevlar in the containment belt. The honeycomb section was backed with two plies of Kevlar/epoxy to provide additional case stiffness to minimize the out-of-roundness which develops during the containment process. Four all-titanium blades were mounted behind each test blade. The blades were released at 5000 rpm providing about 10,300 foot pounds per blade impact energy. Both blades were fully nested in the honeycomb outside the path of the rotor blades. The first two trailing blades were bent over the outer inch of the span indicating some inter-

action with the released blades during the initial phase of the containment process. There was no Kevlar pullout or other significant interaction between the remaining rotor blades and the containment system. The deceleration was smooth and the rotor could be easily turned by hand following the test.

The fourth test utilized only one trailing blade since the containment system had no provisions for nesting blade debris. Inspection of the films revealed that the test blades penetrated into the containment system immediately following the release without interacting with the trailing blade. The released blades then rebounded back into the rotor path and were struck by the opposite trailing blade and a very strong interaction developed among the rotor blades, the released debris fragments, and the containment system. The resulting interaction dragged out the Kevlar which fractured the trailing blades at the base of the airfoil. One of these fragments impacted a region which had little Kevlar remaining and escaped the containment system. The first witness plate was dented but not penetrated by the escaped blade fragment. Figure 13 shows the test rotor and containment system before and after this test.

The penetration and containment data obtained from the rotating impact tests were reduced and are plotted with the gas gun test data on Fig. 14. Only the data from the honeycomb specimens are shown. Since only partial penetration of the Kevlar section of the containment system was experienced, the penetration threshold should fall considerably below the value used in the design of the rotational test specimens. The estimated location of the penetration threshold is indicated by the lower line which corresponds to a value of the constant of 0.00265. These tests completed the experimental part of the initial program conducted under contract NAS320118.

DESIGN REFINEMENT AND EVALUATION

The initial program test results established the effectiveness of the Kevlar belt containment concept and demonstrated the necessity of providing trajectory control and nesting provisions for fan blade debris.

A second program conducted under contract NAS 3-21823 was undertaken to further refine the optimization of the Kevlar belt containment concept. Table III presents the primary features of the program. Twenty blade impacts are specified. Dual blade releases were involved in all but two runs. Two fully bladed tests each involving a single blade release, were specified for the remaining tests. Both all-titanium and superhybrid composites blades were tested with heavy emphasis on the all-titanium blades.

The containment concepts investigated are presented schematically in Fig. 15. The metal face sheets were 0.016-inch thick 305 stainless steel and the back sheets were 0.032-inch 2024-T3 aluminum. A 0.026-inch (2 ply) layer of Kevlar/epoxy was bonded to the honeycomb section. Two 360 degree specimens were fabricated for the fully bladed rotor tests. The remaining 18 specimens were 180 degree segments which were attached to vertically opposite hard points on the test rig as in the previous program. Specimens with and without Kevlar felt combined with the Kevlar cloth were tested. Two weaves of Kevlar cloth, one bi-directional (#328) and one unidirectional (#143) were included. Both free and rigidly attached cloth edge retention concepts were tested. The free edge condition consisted of a simple stacking of the Kevlar cloth layers. The rigid edge condition was obtained by impregnating the edges of the Kevlar layers with epoxy to create a stiffened edge band which was drilled with 0.25-inch diameter holes spaced on 1-inch

centers. Differing degrees of edge restraint were achieved by using all bolt holes every other bolt hole or every forth bolt hole.

The tests were divided into two series. The initial test series is summarized in Table IV. In all cases the released impact fragments remained within the containment system. In the higher energy tests, 6 through 10, the outer cover of the containment system was deflected sufficiently to contact and dent the first 0.25-inch thick aluminum witness plate. On tests 8, 9, and 10 the root section of the released blade completely penetrated the outer case but the airfoil section of the blades remained embedded in the Kevlar cloth. Figure 16 presents the series I test data. If threshold containment is evaluated by the partial perforations of tests 8, 9, and 10, a reduction of about 65 percent in the Kevlar thickness requirement is obtained. The addition of the Kevlar felt in tests 9 and 10 did not appear to have any significant effect on the containment process or the damage sustained by the containment system. Evaluation of the second series of tests was incomplete at the time specified for submission of this paper. It is not expected that the remaining tests will significantly change the evaluation of the Kevlar containment characteristics.

CONCLUSIONS

At the present time, the tentative design thickness for a Kevlar belt containment system would probably be based on the thickness required to prevent any rupture of the outer layer of the containment structure. This condition appears to be conservatively defined by a value of the energy correlation constant in Eq. (1) of 0.00125. A design study which applied this criterion to a potential CF6 engine application established that a containment system weight reduction of 18 percent could be expected. Design refinement, possible when the Kevlar system is incorporated into an original engine design, is expected to provide a 30 percent weight reduction.

REFERENCES

1. Stotler, C. L. and Coppa, A. P., "Containment of Composite Fan Blades," NASA CR-159544, July 1979.

2. Chamis, C. C., Lark, R. F., and Sullivan, T. L., "Boron/Aluminum-Graphite/Resin Advanced Fiber Composite Hybrids," NASA TN D-7879, February 1975.

TABLE I. - PROJECTILE IMPACT TESTING SUMMARY.

TEST NO.	CONTAINMENT CONCEPT	lb W_p	fps V	ft-lb K.E.	lb/ft^2 B	ft^3 K.E./B	PROJECTILE TYPE	COMMENTS
1	STEEL	0.1281	850	1437	2.965	485	TITANIUM	REDIRECTED
2	STEEL	0.1281	912	1654	2.965	558	TITANIUM	REDIRECTED
3	STEEL	0.0675	897	843	2.965	284	SUPERHYBRID	SHATTERED
4	STEEL	0.1281	876	1526	2.965	515	TITANIUM	REDIRECTED
5	ALUMINUM/KEVLAR	0.0675	735	566	1.456	389	SUPERHYBRID	CAUGHT
6	ALUMINUM/KEVLAR	0.1281	634	800	1.456	549	TITANIUM	CAUGHT - KEVLAR PULLED OUT
7	HONEYCOMB	0.1281	920	1684	2.070	814	TITANIUM	PUNCTURED - ESCAPED
8	HONEYCOMB	0.1281	940	1758	2.070	849	TITANIUM	PUNCTURED - ESCAPED
9	TITANIUM FINNED	0.0675	940	926	3.429	270	SUPERHYBRID	CAUGHT - SLIT PROJECTILE
10	TITANIUM FINNED	0.1281	940	1758	3.429	513	TITANIUM	CAUGHT
11	KEVLAR FINNED-LONG	0.1281	940	1758	3.407	516	TITANIUM	PUNCTURED - ESCAPED
12	KEVLAR FINNED-LONG	0.0675	940	926	3.407	272	SUPERHYBRID	CAUGHT - SLIT PROJECTILE
13	ALUMINUM FINNED	0.1281	940	1758	3.471	506	TITANIUM	PUNCTURED - ESCAPED
14	ALUMINUM FINNED	0.1281	762	1155	3.471	333	TITANIUM	CAUGHT
15	KEVLAR FINNED-SHORT	0.1281	940	1758	3.345	526	TITANIUM	CUAGHT
16	KEVLAR FINNED-SHORT	0.0675	940	926	3.345	277	SUPERHYBRID	CAUGHT - SLIT PROJECTILE
17	STEEL/ KEVLAR-THICK	0.1281	770	1179	579	579	TITANIUM	CAUGHT
18	STEEL/ KEVLAR-THICK	0.1281	940	1758	2.038	863	TITANIUM	PUNCTURED - CAUGHT- KEVLAR PULLED OUT
19	STEEL/ KEVLAR-THIN	0.1281	767	1170	1.826	641	TITANIUM	PUNCTURED - CAUGHT BARELY - KEVLAR PULLED OUT
20	STEEL/ KEVLAR-THIN	0.1281	723	1040	1.826	570	TITANIUM	PARTIAL PUNCTURE - CAUGHT

W_p - BLADE PROJECTILE WEIGHT; V - PROJECTILE IMPACT VELOCITY; K.E. - PROJECTILE KINETIC ENERGY; B - CONTAINMENT STRUCTURE WEIGHT PER UNIT AREA

TABLE II. - SPIN IMPACT TEST PLAN - NAS3-20118

TEST NUMBER	CONTAINMENT GEOMETRY		IMPACTING BLADE	FAN SPEED, RPM
	NUMBER OF KEVLAR PLIES	NESTING FEATURES		
1 RHS	22	180^0 AL HONEYCOMB	COMPOSITE	5000
1 LHS	22	NONE	COMPOSITE	5000
2 RHS	22	180^0 AL HONEYCOMB	COMPOSITE	5000
2 LHS	22	NONE	COMPOSITE	5000
3 RHS	29	180^0 AL HONEYCOMB	TITANIUM	5000
3 LHS	29	NONE	TITANIUM	5000
4 RHS	29	NONE	TITANIUM	5000
4 LHS	29	NONE	TITANIUM	5000

EACH TEST CONSISTED OF RELEASE OF TWO BLADES, 180^0 APART, INTO TWO DISTINCT CONTAINMENT SYSTEMS SEGMENTS.

RHS - RIGHT HAND SIDE
LHS - LEFT HAND SIDE

TABLE III. - SPIN IMPACT TEST PLAN
(NUMBER OF TESTS)

CONTAINMENT SYSTEM VARIABLES		IMPACT FRAGMENT VARIABLES					
		MATERIAL	TITANIUM AIRFOIL		TITANIUM BLADE		COMPOSITE AIRFOIL
KEVLAR BELT THICKNESS	KEVLAR EDGE CONDITION	MASS	M		M_2		M_3
		VELOCITY	V_1	V_2	V_3	V_4	V_5
t_1	FREE		1	1	1	1	1
t_2	FREE		1	2*	1	2*	
t_3	FREE				1	1	
t_4	FREE						1
t_4	BOLTED 1 inch spacing				1	1	
t_4	BOLTED 2 inch spacing				1	1	
t_4	BOLTED 3 inch spacing				1	1	

*ONE TEST WILL BE SINGLE RELEASE OUT OF A FULLY BLADED ROTOR INTO A 360 DEGREE TARGET. ALL OTHER TESTS WILL BE DOUBLE RELEASE WITH THREE TRAILING BLADES INTO 180 DEGREE TARGETS.

TABLE IV. - IMPACT TEST PARAMETERS - FIRST TEST SERIES

No.	PLIES OF DRY KEVLAR	RELEASED Wt. - Lbs.	ROTOR SPEED - RPM	KINETIC ENERGY - ft-Lb
1	12	1.355	4500	8400
2	8	1.311	4500	8127
3	12	1.355	5000	10,370
4	8	1.264	5000	9674
5	12	2.330	5000	13,275
6	8	2.341	5000	13,275
7	12	2.335	5285	14,794
8	8	2.335	5285	14,794
9	8	2.267	5300	14,445
10	8	2.293	5300	14,610

PLUS 0.20 of 3.5 lb/ft^3 KEVLAR FELT

Figure 1. - Gas gun containment system test facility.

Figure 2. - Containment system test specimen.

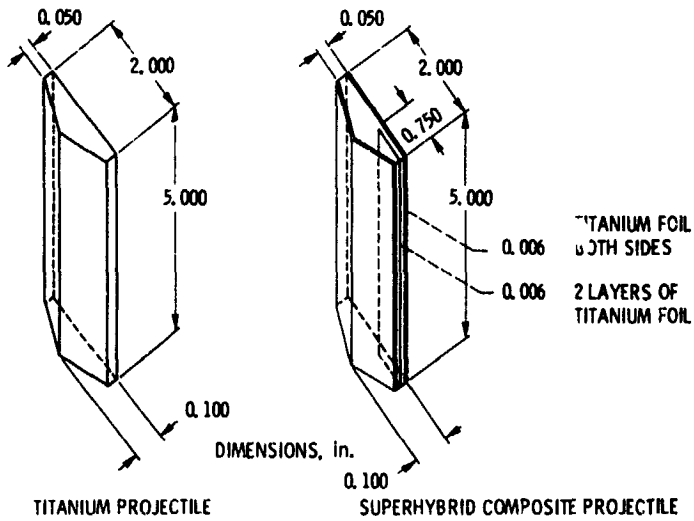

Figure 3. Simulated blade fragment gun projectiles.

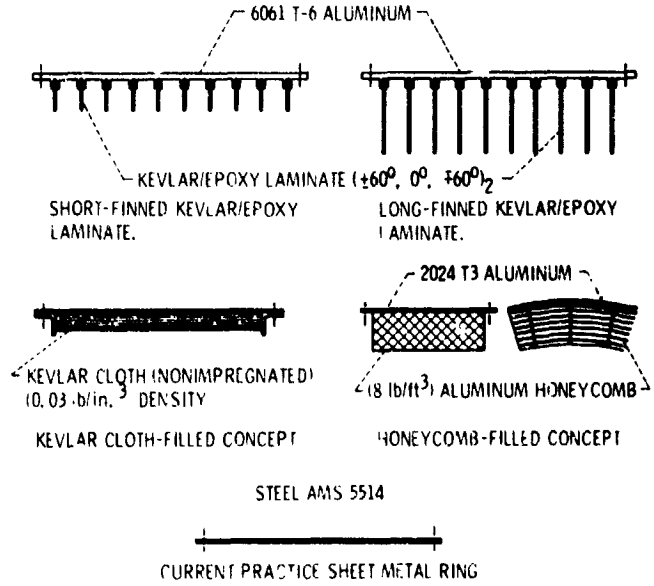

Figure 4. Containment concepts evaluated by gas gun impact tests.

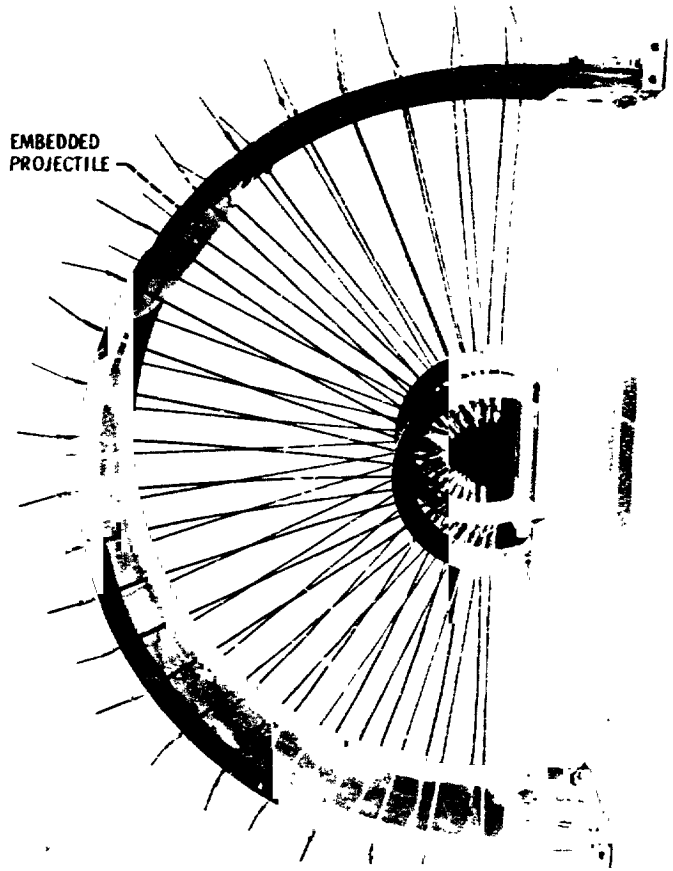

Figure 5. - Superhybrid projectile containment by Kevlar belt target.

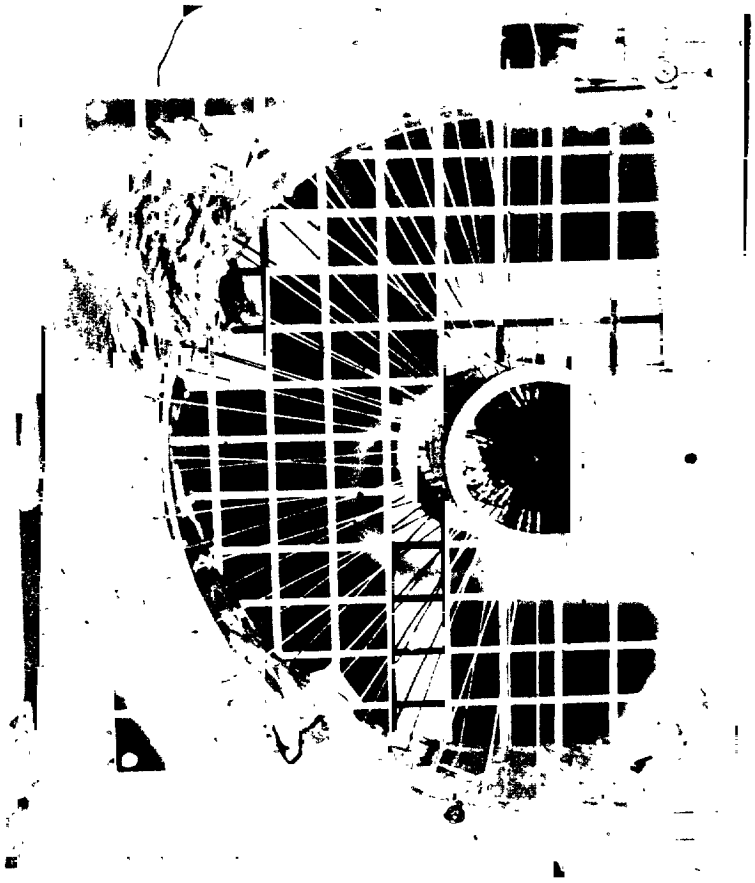

Figure 6. - Incipient penetration of Kevlar belt containment system target.

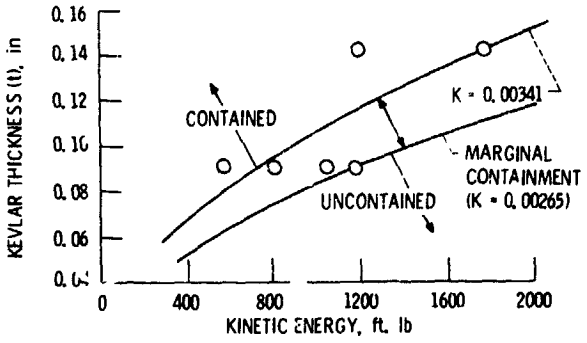

Figure 7. Gas gun impact energy for kevlar belt specimens.

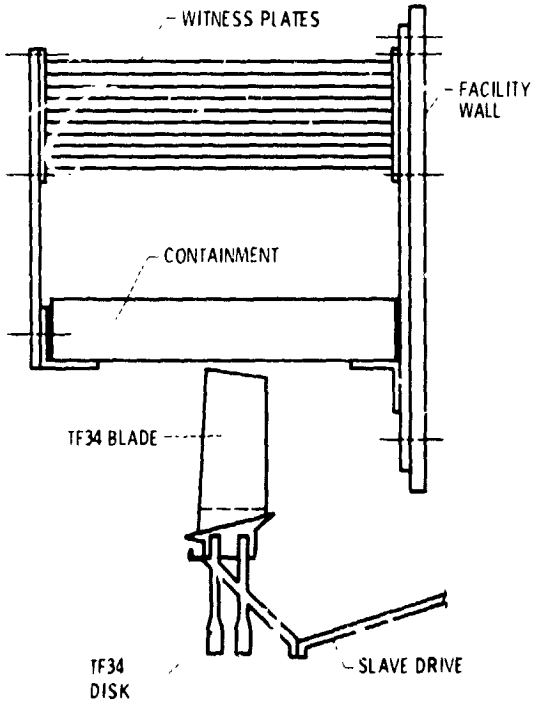

Figure 8. Spin impact test set up.

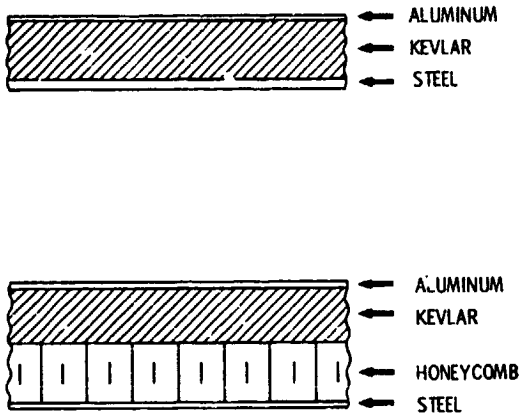

Figure 9. Kevlar belt containment concepts.

Figure 10. - Typical spin impact test set up.

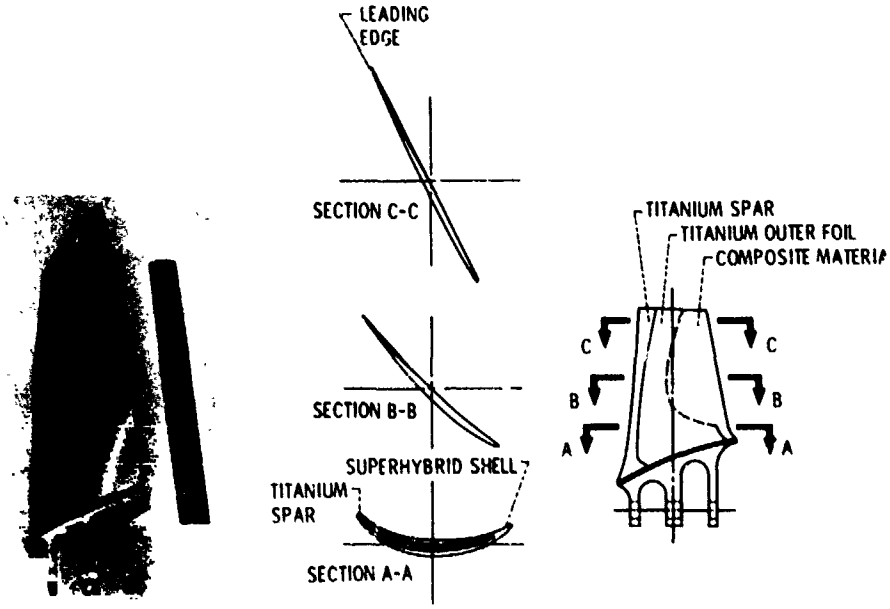

Figure 11. - Blades impacted into containment test specimens.

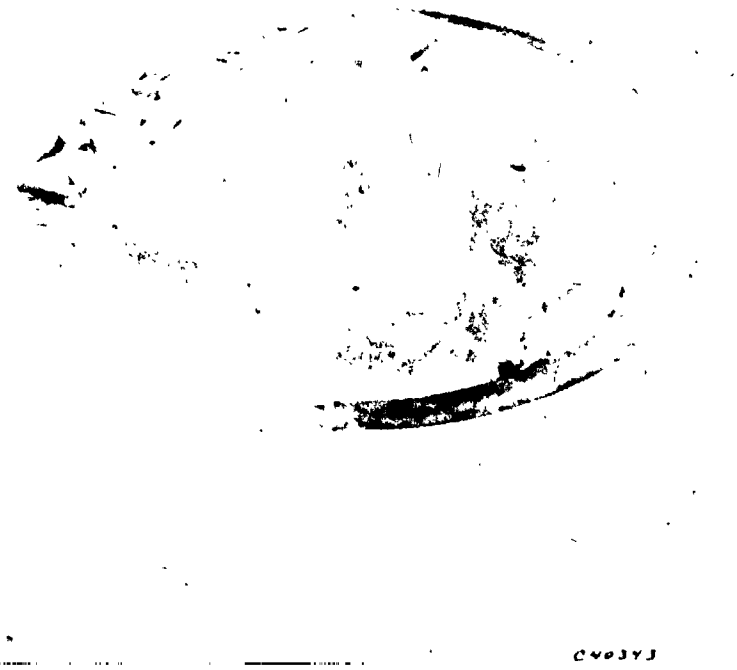

Figure 12. - Containment specimens following impact test no. 1.

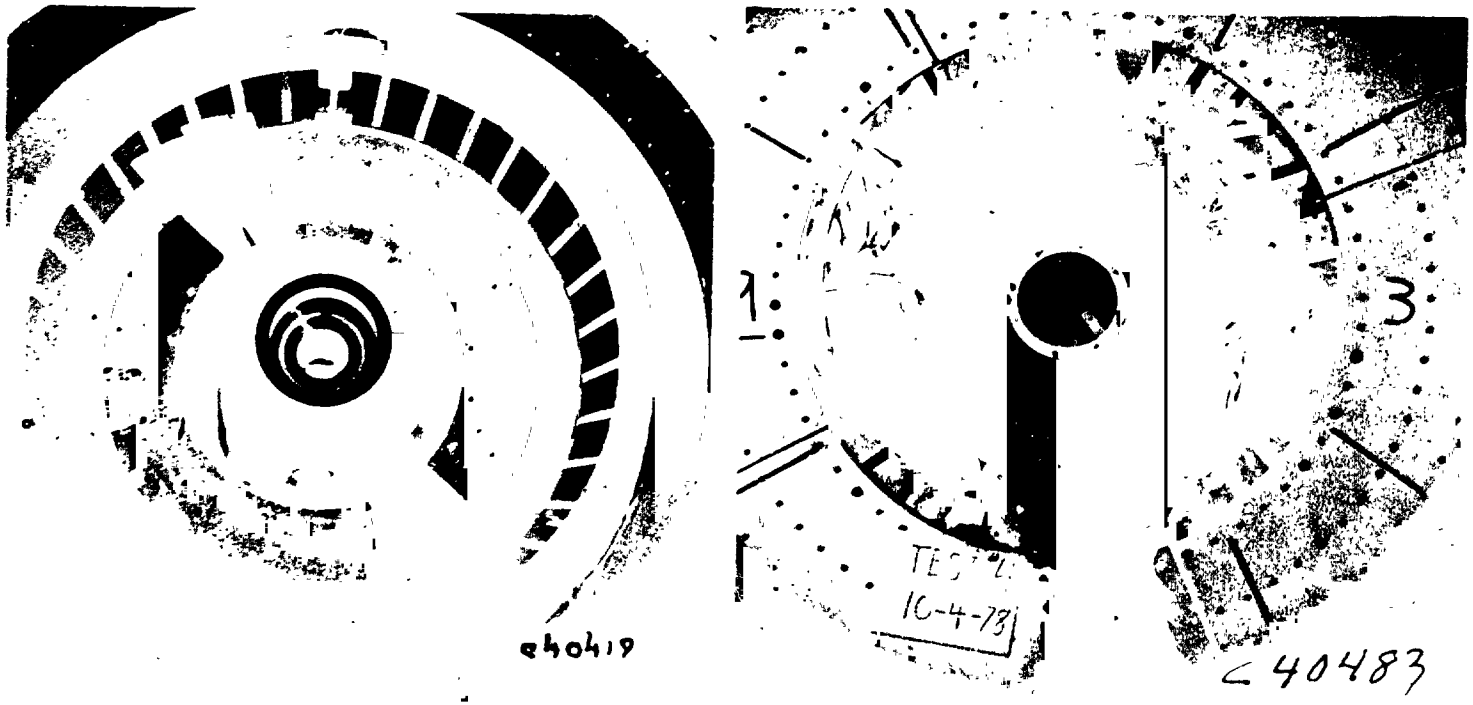

WHIRLIGIG TEST SETUP BEFORE TEST 4

CONTAINMENT TEST 4 FOLLOWING IMPACT

Figure 13. - Rebound and subsequent interaction damage due to lack of nesting.

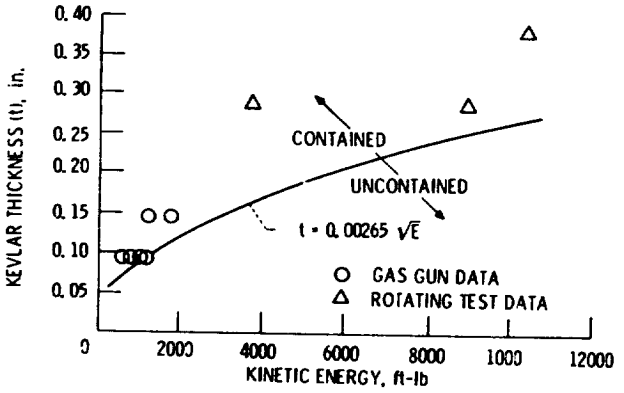

Figure 14. Impact data for kevlar belt/al honeycomb specimens.

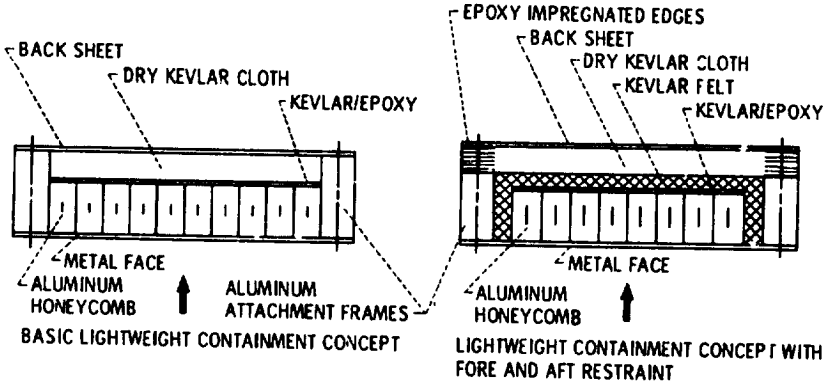

Figure 15. Containment concepts investigated for optimized design.

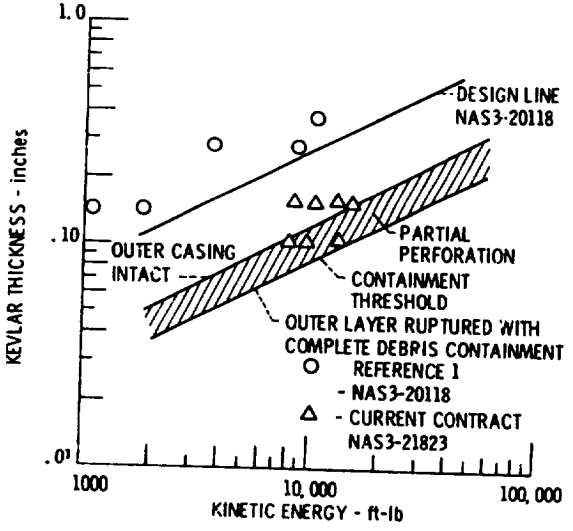

Figure 16. Kevlar belt/Al honeycomb design curves and data.